An information theoretic approach to insulin sensing by human kidney podocytes.

Robert JP Pope[1], Kathryn L Garner[1], Margaritis Voliotis[2], Abigail C Lay[1], Virginie MS Betin[1], Krasimira Tsaneva-Atanasova[2], Gavin I Welsh[1], Richard J M Coward[1] and Craig A McArdle[1,3]

[1]Bristol Renal, Bristol Medical School, University of Bristol, Bristol, BS13NY, UK. [2]College of Engineering, Mathematics and Physical Sciences, Living Systems Institute, University of Exeter, Exeter, EX44QF, UK. [3]Labs. For Integrative Neuroscience and Endocrinology, Bristol Medical School, University of Bristol, Bristol, BS13NY, UK.

Address for correspondence: Prof. Craig A McArdle, Laboratories for Integrative Neuroscience and Endocrinology, Bristol Medical School, University of Bristol, Bristol, BS13NY, UK. Tel: 0044 117 3313077. e-mail:craig.mcardle@bristol.ac.uk

Funding: The work was supported by Kidney Research UK Grant (RP-024-20170302) awarded to C.A.M., G.I.W. and R.J.M.C.

Running title: information theoretic approach to insulin sensing by podocytes

Disclosure: the authors have no conflicts of interest to declare.

HIGHLIGHTS

- Podocytes are insulin-responsive cells that can become insulin-resistant, causing kidney disease with features of diabetic nephropathy.
- Information theory-derived statistics can measure information flow in cells, providing a novel approach to insulin sensing.
- Using this approach in human podocytes, we show that insulin acts via noisy communication channels with most information lost through signaling.
- This loss is mitigated by sensing multiple effectors and response trajectories, and the system is robust to manipulating feedforward signaling but sensitive to inhibition of negative feedback.
- Understanding how system features influence information transfer via insulin receptors may help understanding of kidney disease and inform its treatment.

ABSTRACT

Podocytes are key components of the glomerular filtration barrier (GFB). They are insulin-responsive but can become insulin-resistant, causing features of the leading global cause of kidney failure, diabetic nephropathy. Insulin acts via insulin receptors to control activities fundamental to GFB integrity, but the amount of information transferred is unknown. Here we measure this in human podocytes, using information theory-derived statistics that take into account cell-cell variability. High content imaging was used to measure insulin effects on Akt, FOXO and ERK. Mutual Information (MI) and Channel Capacity (CC) were calculated as measures of information transfer. We find that insulin acts via noisy communication channels with more information flow to Akt than to ERK. Information flow estimates were increased by consideration of joint sensing (ERK and Akt) and response trajectory (live cell imaging of FOXO1-clover translocation). Nevertheless, MI values were always <1Bit as most information was lost through signaling. Constitutive PI3K activity is a predominant feature of the system that restricts the proportion of CC engaged by insulin. Negative feedback from Akt supressed this activity and thereby improved insulin sensing, whereas sensing was robust to manipulation of feedforward signaling by inhibiting PI3K, PTEN or PTP1B. The decisions made by individual podocytes dictate GFB integrity, so we suggest that understanding the information on which the decisions are based will improve understanding of diabetic kidney disease and its treatment.

KEYWORDS.

insulin receptor, podocyte, diabetes, phosphatidyl-inositol 3 kinase (PI3K), mutual information, cell signaling.

GRAPHICAL ABSTRACT.

An information theoretic approach to insulin sensing by human kidney podocytes.

Background: Insulin acts on podocytes to protect the glomerular filtration barrier but information is lost through signaling and information transfer has not been quantified in these cells.

It can be measured statistically, taking into account cell-cell variation that impairs information transfer.

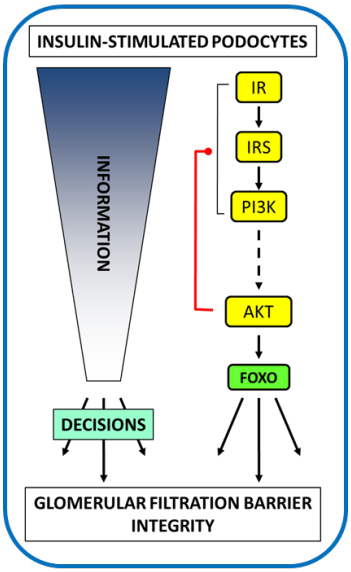

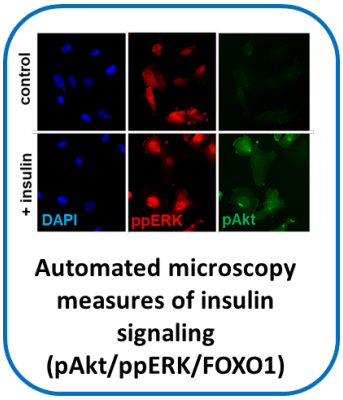

Automated microscopy measures of insulin signaling (pAkt/ppERK/FOXO1)

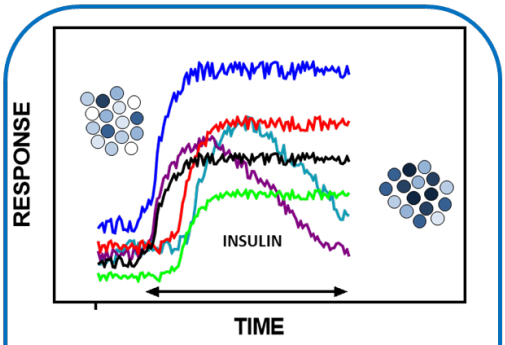

Responses vary markedly from cell-to-cell. This noise and leak (constitutive activity) impairs hormone sensing.

Conclusions: Insulin acts via noisy channels with most information lost through signaling. However, this loss is mitigated by dual sensing, by sensing responses over time and by negative feedback in the insulin signaling network.

INTRODUCTION.

Podocytes are a crucial component of the glomerular filtration barrier (GFB). They interdigitate with one-another to form a filter that is permeable to water and other small molecules from the blood, but not to proteins such as albumin. The appearance of albumin in the urine is a hallmark of kidney disease (1) and the essential role of podocytes in GFB integrity is illustrated by the fact that more than 60 human genetic mutations causing albuminuria all encode proteins with specific roles in podocytes (2). Diabetic nephropathy is the leading cause of kidney failure globally, accounting for approximately half of patients entering end stage renal failure in the USA (United States Renal Data System. 2013 Atlas of End-Stage Renal Disease, https://www.usrds.org/2013/pdf/v2_ch1_13.pdf (2013)). It is classically characterised by progressive albuminuria due to GFB damage that primarily reflects impaired podocyte function (3). It was attributed to hyperglycaemia but we have shown that podocytes are insulin-sensitive and that rendering the podocyte insulin resistant also causes nephropathy in normoglycaemic conditions (4-6), suggesting podocyte insulin resistance is important in this condition. This has focussed research onto direct insulin effects on podocytes, and the possible therapeutic benefit from modulating insulin receptor (IR) signaling in them. In podocytes, IR engage the canonical IR/phosphatidylinositol 3-kinase (PI3K)/Akt signaling network (7) to drive activities including glucose uptake and cytoskeletal remodelling, both of which are important for GFB integrity (8).

Insulin sensitivity is a key concept in diabetology that initially related to the effectiveness of insulin at clearing glucose from the blood but also applies to insulin-stimulated responses in in vitro assays. Recent cell biology studies highlight an entirely different approach to assessment of hormone sensing based not on the size of the response, but on the reliability with which stimuli can be inferred from responses. Consider an experiment in which equal numbers of cells are exposed to one of 8 insulin concentrations and a response (i.e. Akt activation) is measured. If the insulin concentration can be inferred precisely from the response, insulin must have acted via a hi-fidelity channel with no information lost through signaling. Alternatively, it might only be possible to infer that the cells have or have not been exposed to insulin. In this case we would conclude that most information has been lost because the input was 3Bits (2^3=8 insulin concentrations) whereas at most 1Bit (with or without insulin) could be inferred from the response. Information transfer can be quantified more precisely with statistical measures

including Channel Capacity (CC), which represents the maximal number of environmental states that the receiver can discriminate, and Mutual Information (MI) that measures the quality of inference of stimulus from response. Both are measured in Bits, where a CC of 1Bit means that the receiver can unambiguously discriminate two different environmental states (9-16).

This approach was developed for electronic communication systems but has more recently been applied to sensing of growth factors, cytokines and hormones (9-16). This involves measurement of responses in large numbers of individual cells, enabling information transferred through signaling pathways to be calculated, taking into account cell-cell variation (9-16). In essence, the reliability with which individual cells sense environment features is calculated taking into account not only the size of the response, but also the noise in the system. This has revealed that there is typically marked loss of information through cell signaling pathways, although such loss can be mitigated by sensing of multiple effectors (12,17,18) and by sensing response trajectories (13,14,19-21). More generally, this novel approach can be used to explore how system architecture influences information flow, but it has not been applied to podocytes. Here, we measure IR-mediated information transfer in hPod cells (a human podocyte cell line) and find that it is low but can be increased by joint sensing (of pAkt and ppERK) and by sensing responses over time. Surprisingly, IR-mediated information transfer was robust to manipulation of feedforward signaling and constitutive PI3K/Akt activity was identified as a prevalent feature that limits IR-mediated information transfer. Interestingly, we find that Akt-mediated negative feedback supresses this constitutive activity and thereby actually improves insulin sensing. We suggest that understanding how system features influence information transfer via IR will be of value in understanding diabetic kidney disease and its treatment.

MATERIALS AND METHODS.

Antibodies and reagents. Primary antibodies (Cell Signaling Technology) were mouse anti-Akt (#2920), rabbit anti-pAkt(S473) (#4060), rabbit anti-pAkt(T308) (#13038), mouse anti-ERK1/2 (#4696) and rabbit or mouse anti-ppERK1/2 (#4370 and 5726). Secondary antibodies (Invitrogen) were goat anti-rabbit Alexa Fluor 488 or 647 (A11008 and A21245) and goat anti-mouse 647 (A21236). EGF was from Sigma (E9644). Insulin, wortmannin, (PI3K inhibitor, #1232)), LY294002 (PI3K inhibitor, #1130)), GSK694002 (Akt inhibitor, #4144), PD184352 (MEK/ERK inhibitor, #PZ0181) GF109203X (PKC inhibitor, #0741), PP2 (Src inhibitor, #1407), SF1670 (PTEN inhibitor, #5020) and CX08005 (PTP1B inhibitor, #6144) were from R&D Systems. Culture reagents were from Sigma Aldrich. DAPI (D1306) and Hoechst 33342 (H3570) were from Thermo Fisher Scientific. pLenti Foxo1 Clover was a gift from Peter Rotwein (Addgene plasmid #67759; http://n2t/addgene:67759 ; RRID:Addgene_67759).

Culture and stimulation. Conditionally immortalised human podocytes expressing IR (hPods) were cultured, seeded into 96 well plates and differentiated for 10-14 days at 37^{o}C as described (4,22,23). For treatments, they were serum starved for 4 hr in 100 µl RPMI-1640 at 37^{o}C and then stimulated with insulin or EGF. hPod/FOXO1 cells are hPods transduced with recombinant lentivurus for expression of FOXO1-clover (24). Transduced cells were selected with puromycin (0.8 µg/ml) and transduction efficiency was >98%.

Fluorescence staining and high content imaging. Cells were fixed and stained as described (23,25), using antibodies at 1:200 except anti-pAkt (T308) which was 1:800. For most experiments nuclei were stained with DAPI (25). Cells were imaged with an InCell Analyzer 2200 (GE Healthcare) using a 10X objective and with LED/filter combinations for DAPI (blue channel), Alexa488 (green channel) or Alexa647 (red channel). For live cell experiments, hPod/FOXO1 cells were processed as above except that 30 min before imaging, the media was replaced with live cell imaging buffer (20,26) containing 2 µM Hoechst 33342 to stain nuclei. Treatments were added to wells (25 µl at 5X concentration added to 100 µl medium) before transferring plates to the (pre-heated) InCell stage for imaging at 37^{o}C.

Statistics. Treatments were in 2-4 wells with 1-4 fields per well, providing 2000-10000 imaged cells for each treatment in each experiment. Image analysis with InCell Analyzer Workstation Multi-Target Analysis algorithms provided fluorescence intensity (in arbitrary fluorescence units, AFU) in the nucleus and cytoplasm (20,25). For the FOXO1-clover translocation assays a cut-off was used, defining cells as +ve when cytoplasmic FOXO1-clover >20% higher than in the nucleus. Alternatively, the cytoplasmic fraction (FOXO1-CF) was calculated. For the live cell experiments, individual cells were tracked as described (20).

For most experiments, individual cell measures from complete concentration-response curves were used to calculate MIs using MatLab (13,20,27) and the following formula:

$$I(Z;S) = H(Z) - H(Z \mid S)$$

where I is the MI between a signal (S) and a response (Z), H(Z) is the unconditional entropy of the response, and $H(Z \mid S)$ is the conditional entropy, and for our analyses S had a uniform distribution (4). This analysis employs a K-Nearest Neighbours (K-NN) approach with K (number of nearest neighbours) set at 6-20 after preliminary estimates showed that it had little influence on calculated MI values within this range.

Where two measures were available for the same cells, we also calculated joint MI between insulin and the paired outputs as above, but with response (Z) now interpreted as a two-dimensional vector.

For hPod/FOXO1 cell experiments, Statistical Learning-based Estimation of Mutual Information (SLEMI) software was used. This algorithm uses a logistic regression model to learn the discrete probability P(S|Z) of the signal (S) given the response (Z) and uses the following (alternative) formula to calculated MI and capacity:

$$I(Z;S) = H(S) - H(S \mid Z).$$

As SLEMI does not use K-NN or binning it is well-suited to highly dimensional outputs and multiple inputs (28) such as the multiple time points in live cell experiments. SLEMI was used to calculate Channel Capacity as well as MI.

For most experiments we report population averaged signalling responses as well as MI and/or CC measures. In each case the values determined from replicate experiments were pooled and are reported as means±SEMs (n=3-6). Statistical significance was then assessed by one- or two-way ANOVA and post-hoc tests as outlined in figure legends.

RESULTS.

Akt is activated by PDK1-mediated phosphorylation at T308 and mTORC2-mediated phosphorylation at S473 (Fig.1). In hPod cells insulin caused concentration-dependent increases in pAkt(T308) and pAkt (S473) (Fig.1, Supplemental Fig.1). Scatter plots revealed marked cell-cell variability (Fig.1D) with this also evident in frequency-distribution plots revealing pAkt(S473) measures to be approximately log-normally distributed (fig.1B). CVs for log pAkt(S473) were 6.0%, 6.5%, 4.7%, 4.9% and 4.8% after 10 min with 0, 10^{-9}, 10^{-8}, 10^{-7} and 10^{-6}M insulin. MI values calculated from single cell measures were ~0.3Bits irrespective of Akt phospho-site (Fig.1F). Five insulin concentrations provide ~2.3Bits of information ($2^{2.3} \sim 5$) so MIs of ~0.3 imply that most information has been lost because of noise (cell-cell variability) in the system. EGF acts on podocytes (29) and also caused concentration-dependent increases in pAkt(S473) and pAkt(T308) with MIs comparable to those for insulin (Fig.1, Supplemental Fig.1D). In cells stimulated 5, 10, 30 or 60 min, population average responses were maximal at 5-10 min and MIs were similar between time-points (Supplemental Fig.2). ppERK and total ERK measurements revealed a modest insulin effect on ppERK, high cell-cell variability and low MIs for ERK activation (maximally ~0.1Bit, Supplemental Fig.2). Thus, although the population averaged data reveal clear concentration-dependent insulin effects, we find that a) individual podocytes are unreliable insulin sensors with most information lost through signaling, b) this is not specific for insulin as there is comparable information transfer via EGF receptors and c) we have not underestimated information flow by poor time-point selection.

Information could be gained by sensing multiple effectors, so we measured pAkt and ppERK in the same cells. MIs for single responses were comparable to those above but were greater when both effectors were considered (0.4-0.5Bits) (Fig.2). The PI3K inhibitor LY294002 reduced population pAkt responses and the MEK inhibitor PD184352 reduced insulin effects on ppERK (Fig.2). LY294002 did not inhibit insulin effects on ppERK and PD184352 did not inhibit insulin effects on pAkt (not shown). PD1845352 had no effect on MIs under any condition and although LY294002 reduced I(pAkt(S473)) and joint sensing, the same tendencies were not significant for pAkt(T308) and ppERK. Thus, information is gained by joint sensing but the increase is modest.

Akt exerts negative feedback on PI3K, but T308 and S473 phosphorylation are both needed for activation, and positive mTORC2-mediated feedback supports S473 phosphorylation (Fig.1G)

(30-33). Akt inhibition (GSK690693) increased basal pAkt (Fig.3) revealing constitutive Akt-mediated negative feedback. The GSK690693 effect on basal pAkt(T308) was greater than its effect on basal pAkt(S473) (Fig.3) which likely reflects inhibition of both negative and positive feedback for pAkt(S473). GSK690693 shifted the concentration-dependent effects of insulin on pAkt and also tended also to reduce the maximal insulin effect on pAkt(S473) (Fig.3). MIs for control pAkt responses were ~0.25Bits and both were significantly reduced by GSK690693 whereas I(ppERK;insulin) was unaltered by GSK690693 (Fig.3C). Thus, we report a novel role for Akt-mediated negative feedback in protecting insulin sensing.

Phosphatase and tensin homolog (PTEN) is a negative regulator of Akt (Fig.1) and PTEN knock-down increases pAkt in mouse podocytes (34). PTEN inhibition (SF1670) increased basal pAkt(S473), but didn't influence cell-cell variability as the CV for log pAkt(S473) (6.8±0.3%, n=3) was not significantly influenced by SF1670 ($P>0.05$ by one-way ANOVA). SF1670 effectively shifted the insulin concentration-response curves upward but didn't alter I(pAkt;insulin) (Fig.4). Protein tyrosine phosphatase 1B (PTP1B) also negatively regulates Akt (Fig.1) and PTP1B knockdown increases Akt activation in mouse podocytes (25). PTP1B inhibition (CX08005) also increased basal pAkt(S473) but did not influence cell-cell variability as the CV for log pAkt(S473) (6.5±0.4%, n=3) was not significantly influenced by CX08005 ($P>0.05$ by one-way ANOVA). This inhibitor also effectively shifted the insulin concentration-response curves upward without altering I(pAkt;insulin) (Supplemental Fig.3B). Similar data were obtained for pAkt(T308) (not shown). Thus, these two major negative regulators do not actually influence information transfer via IR to Akt in this system.

Forkhead box binding protein 1 (FOXO1) translocates to the cytoplasm when phosphorylated by Akt so we expressed FOXO1-clover as a live cell reporter for Akt activation. In hPod/FOXO1 cells insulin increased pAkt(S473) and pAkt(T308) levels and caused cytoplasmic translocation of FOXO1-clover (Fig.5D-F). PI3K inhibition reduced both responses whereas Akt inhibition increased pAkt(T308) in control cells and prevented FOXO1-clover translocation (Fig.5). Without insulin, LY294002 caused small reductions in pAkt(S473) and pAkt(T308) whereas GSK690693 increased both measures. Coefficients of variance for the log pAkt(S473) and pAkt(T308) measures were significantly increased by GSK690693 but were not altered by

LY6942002 (Fig.5 legend), and LY294002 caused a pronounced reduction in cytoplasmic FOXO1-clover (measured using a % +ve cut-off), whereas GSK690693 increased it (Fig.5). Thus, FOXO1-clover translocation is indeed dependent on Akt activity and is particularly sensitive to the low levels of constitutive Akt activity without insulin. MIs were ~0.2, 0.05 and 0.3Bits for pAkt responses, FOXO1-clover translocation and joint sensing, respectively (Fig.5). CC values followed the same trends but were somewhat higher. GSK690693 reduced all these measures whereas LY294002 tended to increase them (Fig.5) reinforcing the conclusion that insulin sensing is relatively robust to PI3K inhibition in podocytes.

Using FOXO1-clover translocation as a live cell readout for Akt activation (Fig.6A), LY294002 and wortmannin both reduced the % FOXO1 +ve cells (half-times 10-15 min). The % FOXO1 +ve increased from ~55% to 75% in control cells, which may reflect mechanical stimulation with medium addition. In control cells ~50% of cells were FOXO1 +ve at time 0 and insulin caused cytoplasmic translocation that was rapid, sustained, and concentration-dependent (Fig.6B). PI3K inhibitor reduced cytoplasmic FOXO1-clover (10-20% FOXO1 +ve at time 0) but did not prevent insulin-stimulated translocation (Fig.6). Similarly, when FOXO1 cytoplasmic fraction (FOXO1 CF) was calculated for tracked cells there was a clear reduction on PI3K inhibition, and insulin stimulated translocation not only in control cells, but also with inhibitor (Fig.7). These data revealed marked cell-cell variability so unsurprisingly, MIs at single time-points were low (<0.1Bit). However, the MI calculated taking trajectories into account was approximately doubled (compare Fig.8A and C). PI3K inhibition increased MIs at most time-points and when trajectories were considered, MI was increased by wortmannin. Similar relationships were seen for CCs, although these were consistently higher than the corresponding MIs (Fig.8). We also explored the possibility that insulin--stimulated FOXO1-clover might reflect activation of PKC, Src or MEK (other kinases activated by IR) but inhibiting these enzymes had no effect on FOXO1-clover distribution whereas GSK690693 ablated the response to insulin with or without wortmannin (Supplemental Fig.4). This re-enforces the conclusion that the translocation assay is sensitive to low levels of Akt activity but most importantly, these data reveal that podocytes do indeed gain information by sensing over time (Fig.8).

We next considered more complex environments, by varying insulin with or without EGF, PI3K inhibitor and MEK inhibitor, measuring pAkt(S473) and ppERK so that CCs could be calculated for sensing all 32 environments or any subset of them. Both stimuli activated both effectors and the pAkt responses were inhibited by LY294002 whereas the ppERK responses were inhibited by PD184352 (Supplemental Fig.5). For all 32 treatments, CCs were ~0.75Bit for pAkt(S473), ~1.0Bit for ppERK and ~1.75Bit for joint sensing (Supplemental Fig.6). These values estimate the information about the multi-dimensional environment that can pass to Akt, to ERK or via the Akt/ERK network, respectively. Additional important observations were that only a proportion of this capacity was engaged by activators (CC with joint outputs and with insulin inputs was only ~0.6Bit and this increased to only ~0.8Bit for sensing insulin and EGF) and that the capacity for inhibitor sensing (~0.7Bit for joint outputs) was as high as for activator sensing.

DISCUSSION

Cell-cell variation is a fundamentally important feature of physiological systems as it is the decisions made by individual cells (i.e. whether to die or divide) that underlie the health and function of multicellular systems (9-16). This is certainly true for kidney function where death and detachment of individual podocytes reduces GFB integrity, and whether cells migrate or expand into the space will influence repair. Moreover, cellular decision making is inherently linked with the amount of information cell transfer regarding their environment. Here we have calculated Mutual Information (MI) between inputs and outputs, and the related metric of Channel Capacity (CC), as statistical measures of information transfer via IR in podocytes (4-6). Our initial observation was that MI values for insulin-stimulated Akt phosphorylation in fixed cells were ~0.2Bits, implying that podocytes are unreliable insulin sensors with most information lost through signaling. This is consistent with other systems as MI and/or CC values of <1Bit have been reported for single time-point measures of EGF, NGF, GnRH, PACAP and TNFα signaling (12,13,18,26). MIs for stimulation of Akt phosphorylation by insulin and EGF were comparable, and values were similar at 5, 10, 30 and 60 min, allaying concern that our low MIs were specific for IR signaling or had been underestimated by routine 10 min stimulations.

However, cells could gain information by sensing multiple responses and supporting this, we found that MIs for joint insulin sensing by pAkt and ppERK (Fig.2) or by pAkt and FOXO1 (Fig.5) were greater than for either alone. Here it is important to recognise that we focus on the amount of information rather than the decisions informed by it. Consider a system in which insulin effects on pAkt and ppERK are perfectly correlated across individual cells such that there is no additional information from sensing both. In this scenario joint sensing would make the system robust to loss of information by selective pharmacological inhibition of either pathway. Nevertheless, the inhibition would still prevent decisions dependent on either the blocked pathway alone, or on concomitant activation of both. The latter scenario is particularly relevant to ERK and Akt signalling as these effectors can provide combinatorial control of cell fate (35).

Another possible explanation for robustness of information transfer to pharmacological inhibition (12) is that changes in population average responses can scale directly with changes in cell-cell variability. This is seen in our data, where averaged insulin effects on pAkt were

consistently reduced by PI3K inhibitors, whereas the inhibitors had little or no effect on MI measures (Figs.2 and 5). There was also no change in MI when PTEN or PTP1B were inhibited, in spite of the fact that both increased pAkt levels without insulin. Akt inhibition also increased pAkt without insulin but this effect was associated with reduced MI values (Figs.3 and 5). Akt inhibition also increased cell-cell heterogeneity in pAkt values (Fig.5) without insulin, whereas inhibition of PI3K, PTEN or PTP1B did not (Figs.4 and 5) so this is a system in which there is a high level of basal PI3K/Akt signaling and constitutive Akt-mediated negative feedback improves information transfer by opposing this constitutive activity and the associated cell-cell variability. High PIP_3 levels exist in unstimulated cells (i.e. NIH3T3 cells, where PDGF increased PIP_3 levels only 4.5-fold, from 0.1 to 0.45 mol %). It is therefore possible that the same holds true for podocytes, with constitutive Akt activity driven by basal PIP_3 levels (36) and although the reasons for the heterogeneity in Akt responses reported here are unknown, cell-cell-variability in PIP_3 levels is an obvious possibility. In related work, we have shown that constitutive activity impairs information flow via EGF receptors to ERK and that ERK-mediated negative feedback supports EGF sensing by inhibiting it (13), and now show a similar relationship the IR/PI3K/Akt pathway, with Akt-mediated negative feedback protecting information flow by opposing constitutive activity (Fig.3). Most importantly, this novel finding, that IR-mediated information transfer is robust to manipulation of feed-forward signaling but sensitive to inhibition of feedback signaling, has potential translational relevance for podocytes, where insulin resistance promotes kidney disease (37).

We also considered multidimensional inputs and outputs and obtained our highest CC estimates when insulin was varied with or without EGF, PI3K inhibitor and MEK inhibitor. With joint outputs and all 32 possible inputs, CC was 1.74Bits. Lower values were obtained for sensing insulin alone (0.57Bits) or for sensing insulin with or without EGF (0.80Bits) and these were comparable to the value obtained for inhibitor sensing (0.70Bits). These issues are likely related, as high constitutive activity in the Akt/ERK network limits the reliability of insulin sensing by ensuring that only ~50% of the network's information carrying capacity is available to activators.

Single time-point data underestimates information transfer where response trajectories are sensed. In the context of cell signaling this reflects the existence of integrative tracking systems

with biochemical responses sensitive to input dynamics (11,13,14,20,38). Addressing this by live cell imaging we found that insulin rapidly increases FOXO1-CF and with snap-shot data, MIs were low (<0.1Bits) (Fig.8), whereas taking trajectory into account increased MI (~0.2Bits) and the same trends were seen with CC measures. The reporter was largely cytoplasmic before stimulation (Figs.5-7), and since FOXO1-CF was reduced by inhibition of PI3K or Akt (but not by inhibition of PKC, Src or MEK), this could reflect basal PI3K/Akt activity and sensitivity of this assay to low pAkt levels. Consequently, partial PI3K inhibition markedly reduced FOXO1-CF without insulin but did not reduce information flow via IR to FOXO1. Indeed, taking trajectory into account, IR-mediated information transfer to FOXO1 was increased by wortmannin (Fig.8). This again has potential translational relevance as many insulin effects reflect Akt-mediated inactivation of FOXO1 (7) and our data indicate the importance of basal, rather than hormone-stimulated, PI3K/Akt signaling in podocytes. Most importantly however, we find that podocytes gain considerable information by sensing responses to insulin over time.

In summary, using this novel information theoretic approach (9-16) we show that insulin acts via noisy communication channels with most information lost through signaling in podocytes although information transfer estimates were increased by joint sensing and by consideration of responses over time. Our data reveal a remarkable robustness of information flow to manipulation of feedforward signaling, but sensitivity to negative feedback. This contrast has potential translational relevance as the effectors and modules having most impact on information transfer may be most likely to cause disease when perturbed. We also identify constitutive PI3K activity as system characteristics important for insulin sensing. It ensures that the cells sense both activators and inhibitors but also impairs insulin sensing and explains why negative Akt-mediated feedback protects insulin sensing.

References

1. Mogensen CE. Microalbuminuria predicts clinical proteinuria and early mortality in maturity-onset diabetes. *N Engl J Med*. 1984;310(6):356-360.
2. Lovric S, Ashraf S, Tan W, Hildebrandt F. Genetic testing in steroid-resistant nephrotic syndrome: when and how? *Nephrol Dial Transplant*. 2016;31(11):1802-1813.
3. Lin JS, Susztak K. Podocytes: the Weakest Link in Diabetic Kidney Disease? *Curr Diab Rep*. 2016;16(5):45.
4. Coward RJ, Welsh GI, Yang J, Tasman C, Lennon R, Koziell A, Satchell S, Holman GD, Kerjaschki D, Tavare JM, Mathieson PW, Saleem MA. The human glomerular podocyte is a novel target for insulin action. *Diabetes*. 2005;54(11):3095-3102.
5. Welsh GI, Hale LJ, Eremina V, Jeansson M, Maezawa Y, Lennon R, Pons DA, Owen RJ, Satchell SC, Miles MJ, Caunt CJ, McArdle CA, Pavenstadt H, Tavare JM, Herzenberg AM, Kahn CR, Mathieson PW, Quaggin SE, Saleem MA, Coward RJM. Insulin signaling to the glomerular podocyte is critical for normal kidney function. *Cell Metab*. 2010;12(4):329-340.
6. Welsh GI, Coward RJ. Podocytes, glucose and insulin. *Curr Opin Nephrol Hypertens*. 2010;19(4):379-384.
7. Haeusler RA, McGraw TE, Accili D. Biochemical and cellular properties of insulin receptor signalling. *Nat Rev Mol Cell Biol*. 2018;19(1):31-44.
8. Garg P. A Review of Podocyte Biology. *Am J Nephrol*. 2018;47 Suppl 1:3-13.
9. Kholodenko B, Yaffe MB, Kolch W. Computational approaches for analyzing information flow in biological networks. *Sci Signal*. 2012;5(220):re1.
10. Voliotis M, Bowsher CG. The magnitude and colour of noise in genetic negative feedback systems. *Nucleic Acids Res*. 2012;40(15):7084-7095.
11. Bowsher CG, Voliotis M, Swain PS. The fidelity of dynamic signaling by noisy biomolecular networks. *PLoS Comput Biol*. 2013;9(3):e1002965.
12. Uda S, Saito TH, Kudo T, Kokaji T, Tsuchiya T, Kubota H, Komori Y, Ozaki Y, Kuroda S. Robustness and compensation of information transmission of signaling pathways. *Science*. 2013;341(6145):558-561.
13. Voliotis M, Perrett RM, McWilliams C, McArdle CA, Bowsher CG. Information transfer by leaky, heterogeneous, protein kinase signaling systems. *Proc Natl Acad Sci U S A*. 2014;111(3):E326-333.
14. Selimkhanov J, Taylor B, Yao J, Pilko A, Albeck J, Hoffmann A, Tsimring L, Wollman R. Systems biology. Accurate information transmission through dynamic biochemical signaling networks. *Science*. 2014;346(6215):1370-1373.
15. Uda S, Kuroda S. Analysis of cellular signal transduction from an information theoretic approach. *Semin Cell Dev Biol*. 2016;51:24-31.
16. Jetka T, Nienaltowski K, Filippi S, Stumpf MPH, Komorowski M. An information-theoretic framework for deciphering pleiotropic and noisy biochemical signaling. *Nat Commun*. 2018;9(1):4591.
17. Brennan MD, Cheong R, Levchenko A. Systems biology. How information theory handles cell signaling and uncertainty. *Science*. 2012;338(6105):334-335.
18. Cheong R, Rhee A, Wang CJ, Nemenman I, Levchenko A. Information transduction capacity of noisy biochemical signaling networks. *Science*. 2011;334(6054):354-358.
19. Voliotis M, Thomas P, Grima R, Bowsher CG. Stochastic Simulation of Biomolecular Networks in Dynamic Environments. *PLoS Comput Biol*. 2016;12(6):e1004923.
20. Garner KL, Voliotis M, Alobaid H, Perrett RM, Pham T, Tsaneva-Atanasova K, McArdle CA. Information Transfer via Gonadotropin-Releasing Hormone Receptors to ERK and NFAT: Sensing GnRH and Sensing Dynamics. *J Endocr Soc*. 2017;1(4):260-277.
21. Voliotis M, Garner KL, Alobaid H, Tsaneva-Atanasova K, McArdle CA. Gonadotropin-releasing hormone signaling: An information theoretic approach. *Mol Cell Endocrinol*. 2018;463:106-115.
22. Saleem MA, O'Hare MJ, Reiser J, Coward RJ, Inward CD, Farren T, Xing CY, Ni L, Mathieson PW, Mundel P. A conditionally immortalized human podocyte cell line demonstrating nephrin and podocin expression. *J Am Soc Nephrol*. 2002;13(3):630-638.
23. Lay AC, Hurcombe JA, Betin VMS, Barrington F, Rollason R, Ni L, Gillam L, Pearson GME, Ostergaard MV, Hamidi H, Lennon R, Welsh GI, Coward RJM. Prolonged exposure of mouse and human podocytes to insulin induces insulin resistance through lysosomal and proteasomal degradation of the insulin receptor. *Diabetologia*. 2017;60(11):2299-2311.
24. Gross SM, Rotwein P. Akt signaling dynamics in individual cells. *J Cell Sci*. 2015;128(14):2509-2519.
25. Garner KL, Betin VMS, Pinto V, Graham M, Abgueguen E, Barnes M, Bedford DC, McArdle CA, Coward RJM. Enhanced insulin receptor, but not PI3K, signalling protects podocytes from ER stress. *Sci Rep*. 2018;8(1):3902.
26. Garner KL, Perrett RM, Voliotis M, Bowsher C, Pope GR, Pham T, Caunt CJ, Tsaneva-Atanasova K, McArdle CA. Information Transfer in Gonadotropin-releasing Hormone (GnRH) Signaling: EXTRACELLULAR SIGNAL-REGULATED KINASE (ERK)-MEDIATED FEEDBACK LOOPS CONTROL HORMONE SENSING. *J Biol Chem*. 2016;291(5):2246-2259.
27. Voliotis M, Garner KL, Alobaid H, Tsaneva-Atanasova K, McArdle CA. Exploring Dynamics and Noise in Gonadotropin-Releasing Hormone (GnRH) Signaling. *Methods Mol Biol*. 2018;1819:405-429.

28. Jetka T, Nienaltowski K, Winarski T, Blonski S, Komorowski M. Information-theoretic analysis of multivariate single-cell signaling responses. *PLoS Comput Biol*. 2019;15(7):e1007132.
29. Reiser J, Sever S, Faul C. Signal transduction in podocytes--spotlight on receptor tyrosine kinases. *Nat Rev Nephrol*. 2014;10(2):104-115.
30. Manning BD, Toker A. AKT/PKB Signaling: Navigating the Network. *Cell*. 2017;169(3):381-405.
31. Cantley LC. The phosphoinositide 3-kinase pathway. *Science*. 2002;296(5573):1655-1657.
32. Taniguchi CM, Emanuelli B, Kahn CR. Critical nodes in signalling pathways: insights into insulin action. *Nat Rev Mol Cell Biol*. 2006;7(2):85-96.
33. Yang G, Murashige DS, Humphrey SJ, James DE. A Positive Feedback Loop between Akt and mTORC2 via SIN1 Phosphorylation. *Cell Rep*. 2015;12(6):937-943.
34. Santamaria B, Marquez E, Lay A, Carew RM, Gonzalez-Rodriguez A, Welsh GI, Ni L, Hale LJ, Ortiz A, Saleem MA, Brazil DP, Coward RJ, Valverde AM. IRS2 and PTEN are key molecules in controlling insulin sensitivity in podocytes. *Biochim Biophys Acta*. 2015;1853(12):3224-3234.
35. Chen JY, Lin JR, Cimprich KA, Meyer T. A two-dimensional ERK-AKT signaling code for an NGF-triggered cell-fate decision. *Mol Cell*. 2012;45(2):196-209.
36. Liu SL, Wang ZG, Hu Y, Xin Y, Singaram I, Gorai S, Zhou X, Shim Y, Min JH, Gong LW, Hay N, Zhang J, Cho W. Quantitative Lipid Imaging Reveals a New Signaling Function of Phosphatidylinositol-3,4-Bisphophate: Isoform- and Site-Specific Activation of Akt. *Mol Cell*. 2018;71(6):1092-1104 e1095.
37. Welsh GI, Hale LJ, Eremina V, Jeansson M, Maezawa Y, Lennon R, Pons DA, Owen RJ, Satchell SC, Miles MJ, Caunt CJ, McArdle CA, Pavenstadt H, Tavare JM, Herzenberg AM, Kahn CR, Mathieson PW, Quaggin SE, Saleem MA, Coward RJ. Insulin signaling to the glomerular podocyte is critical for normal kidney function. *Cell Metab*. 2010;12(4):329-340.
38. Keshelava A, Solis GP, Hersch M, Koval A, Kryuchkov M, Bergmann S, Katanaev VL. High capacity in G protein-coupled receptor signaling. *Nat Commun*. 2018;9(1):876.

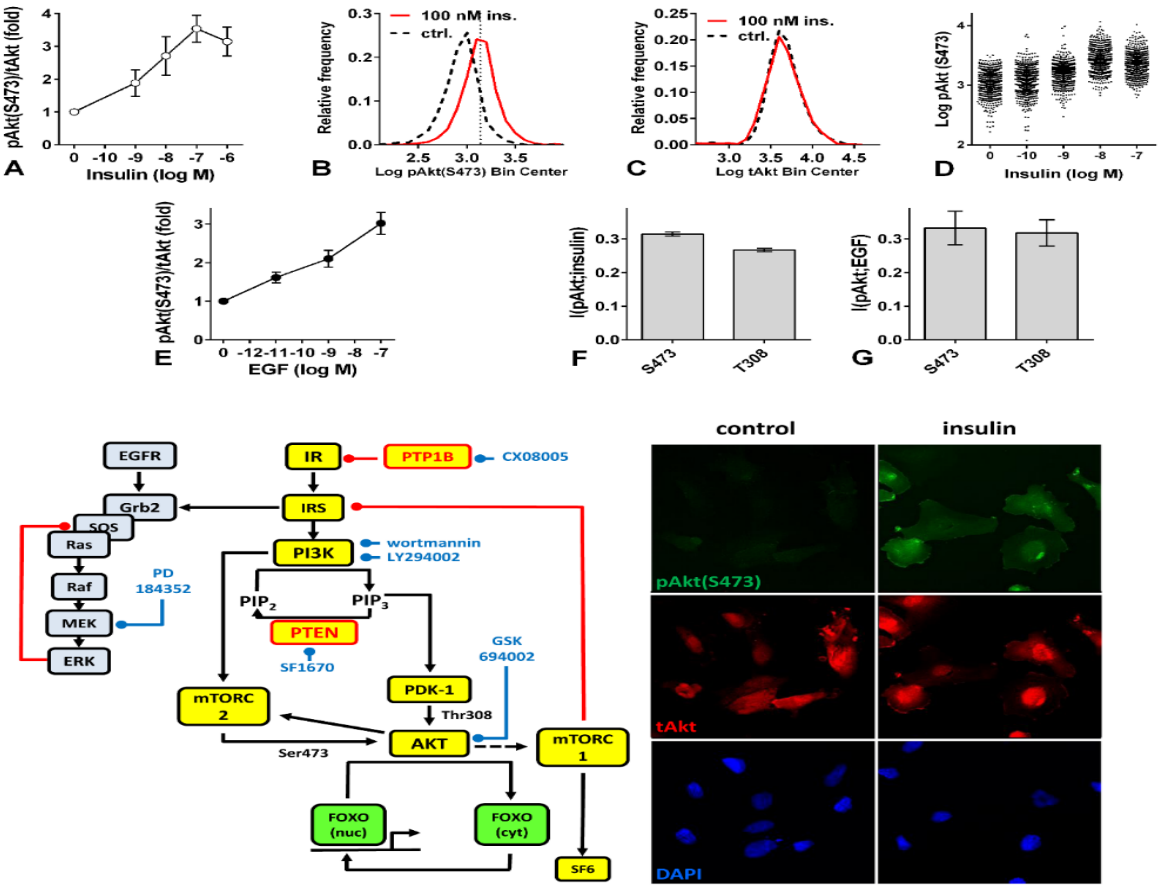

Figure 1. Quantifying IR-mediated and EGFR-mediated information transfer in hPod cells. hPods were stimulated 10 min with the indicated concentrations of insulin (A) or EGF (E). They were then fixed and stained for nuclei (DAPI), pAkt(S473) and total Akt (tAkt) before image acquisition and analysis. Nuclear pAkt measures were normalised to nuclear tAkt and then to the control pAkt/tAkt value (0 insulin, A). Background values (image regions without cells) were not subtracted but gave pAkt/tAkt values of approximately 0.8. B and C show representative frequency distribution plots for individual cells treated with 0 or 10^{-7}M insulin. Nuclear pAkt(S473) and tAkt measures (in arbitrary fluorescence units, AFU) were logged before binning and relative frequencies are plotted against bin centre. Panel D shows scatter plots of single cell log pAkt(S473) measures (1000 cells per treatment in a representative experiment). pAkt(T308) measurements made in parallel are in Supplemental figure 1. Individual cell measures from the complete concentration response curves were used to calculate MIs for insulin-stimulated Akt phosphorylation (I(pAkt;insulin) (E) and EGF-stimulated Akt phosphorylation (I(pAkt;EGF) (F) for the indicated phospho-site. The data in A, E, F and G are means±SEMs (n=4) and for F and G they are expressed in Bits. Lower left is a cartoon for canonical IR/PI3K/Akt and EGFR/Ras/Raf/MEK/ERK signaling as well as the IRS-mediated ERK activation pathway, with the pharmacological inhibitors used shown in blue. The lower right panel shows representative hPod cells treated 10 min with 0 or 10^{-7}M insulin and imaged for pAkt(S473), tAkt or DAPI as indicated.

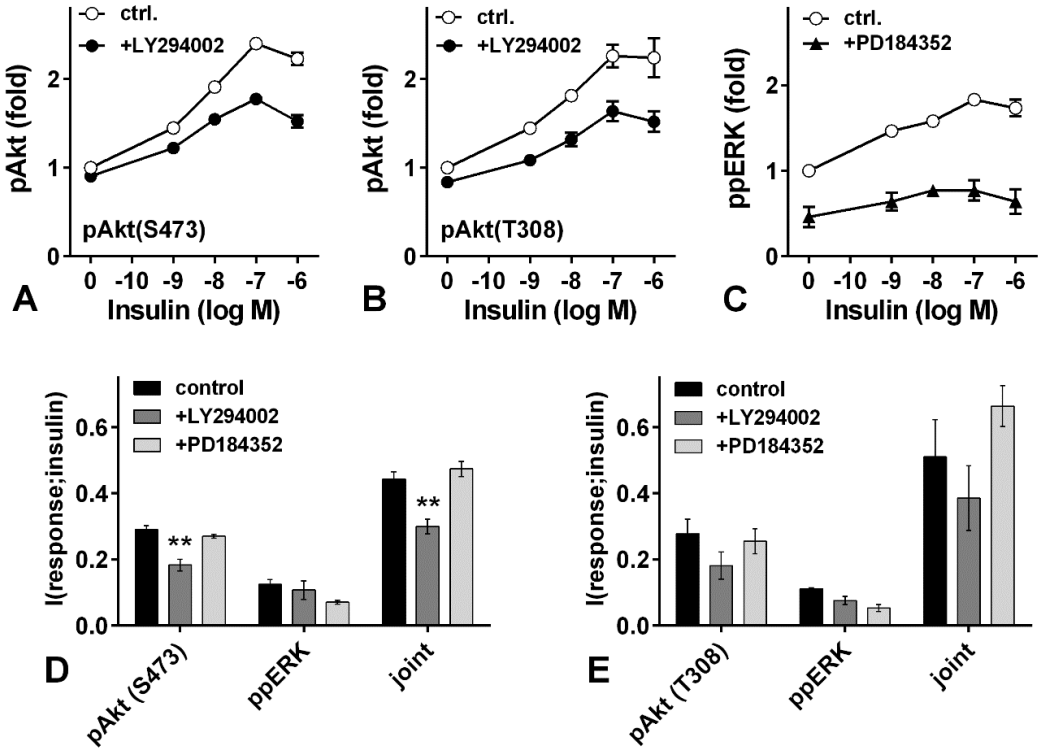

Figure 2. Loss of information is mitigated by joint sensing of pAkt and ppERK in insulin-stimulated hPod cells. A-C: hPods were pre-treated 60 min with or without LY294002 (10^{-5}M) or PD184352 (10^{-5}M) before 10 min stimulation with the indicated concentration of insulin (in the continued presence of inhibitor). The data shown are nuclear pAkt(S473) (A), pAkt(T308) (B) or ppERK (C), normalised to control values from cells receiving no insulin or inhibitor (mean±SEM, n=3). Background values (fluorescence in regions without cells) have not been subtracted but were approximately 0.7 for both pAkt measures and 0.4 for ppERK. D and E: the individual cell measures underlying the concentration response curves were used to calculate MI for insulin-stimulated Akt phosphorylation and ERK phosphorylation as well as the MI for joint sensing of both effectors in the same cells (i.e. for pAkt(S473) and ppERK in D and for pAkt(T308) and ppERK in E). The values shown are means±SEMs for I (response;insulin) in Bits. For D, two-way ANOVA revealed response measured and inhibitor as significant sources of variation and post-hoc tests (Dunnet's multiple comparison) revealed significant differences between control and inhibitor treatment as indicated (**P<0.01). For E, two-way ANOVA revealed the response measured as a significant source of variation, whereas inhibitor was not.

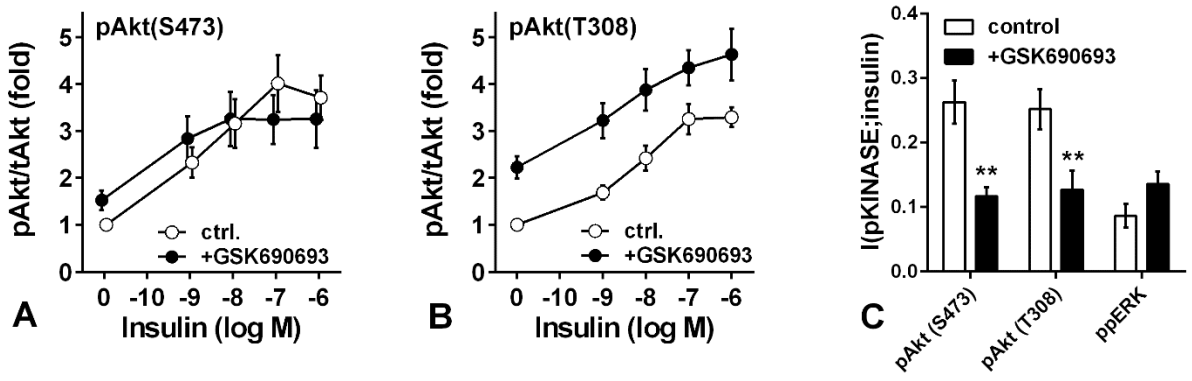

Figure 3. Loss of information is mitigated by Akt-mediated negative feedback in insulin-stimulated hPods. A and B: hPods were pre-treated 60 min with or without the Akt inhibitor GSK690693 ($2x10^{-7}$M) before stimulation for 10 min with insulin (as indicated and in the continued presence of inhibitor). The data are nuclear pAkt(S473) (A) and pAkt(T308) (B) normalised to control values with no insulin or inhibitor (mean±SEM, n=7). Background values have not been subtracted but were ~0.7. The data in A are offset +/- 0.05 log units on the x-axis to aid visualisation of the overlapping error bars. C: MIs for insulin-stimulated Akt phosphorylation in control and GSK690693 treated cells as indicated. In parallel experiments cells treated in the same way were processed for measurement of ppERK and tERK so that MI values for insulin stimulated ERK phosphorylation could also be calculated. The values shown are either I(pAkt;insulin) or I(ppERK;insulin) and are means±SEMs (n=7) in Bits. For C, two-way ANOVA revealed inhibitor as significant source of variation and post-hoc tests revealed significant differences between control and inhibitor treatment as indicated (**P<0.01).

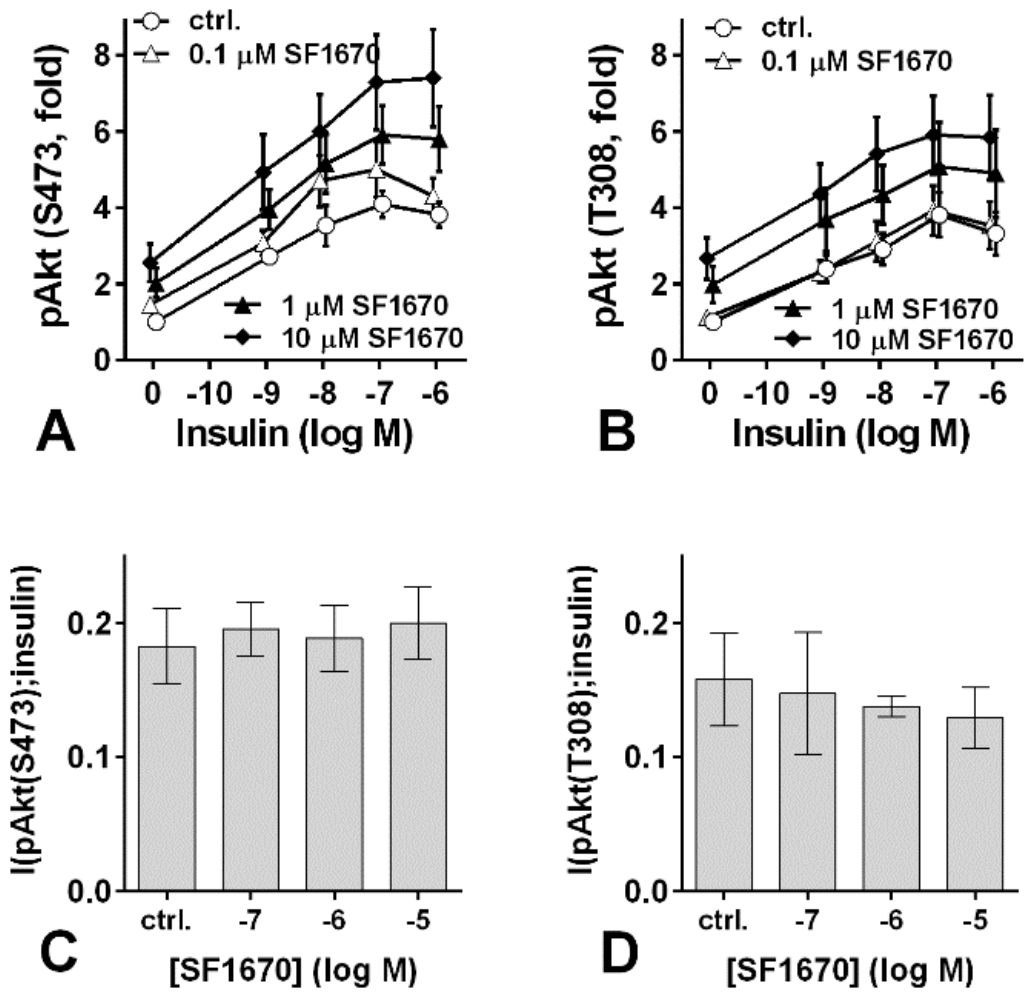

Figure 4. IR-mediated information transfer is not influenced by PTEN inhibition. A and B: hPods were pre-treated for 60 min with or without the PTEN inhibitor SF1670 before 10 min stimulation with insulin (as indicated and in the continued presence of inhibitor). The data shown are nuclear pAkt(S473) (A) or pAkt(T308) (B) normalised to control values in cells receiving no insulin or inhibitor (mean±SEM, n=3). Background values (not subtracted) were ~0.7. Data are offset +/- 0.05 log units on the x-axis to aid visualisation of the overlapping error bars. C and D: individual cell measures were used to calculate MIs for insulin stimulated Akt phosphorylation at S473 (C) or T308 (D). These are plotted against SF1670 concentration (mean±SEM, n=3). Two-way ANOVAs for the data in A and B revealed insulin and inhibitor as significant sources of variation ($P<0.01$ for each) whereas the insulin/inhibitor interaction terms were not significant. One-way ANOVAs for the data in C and D revealed that inhibitor concentration was not a significant source of variation.

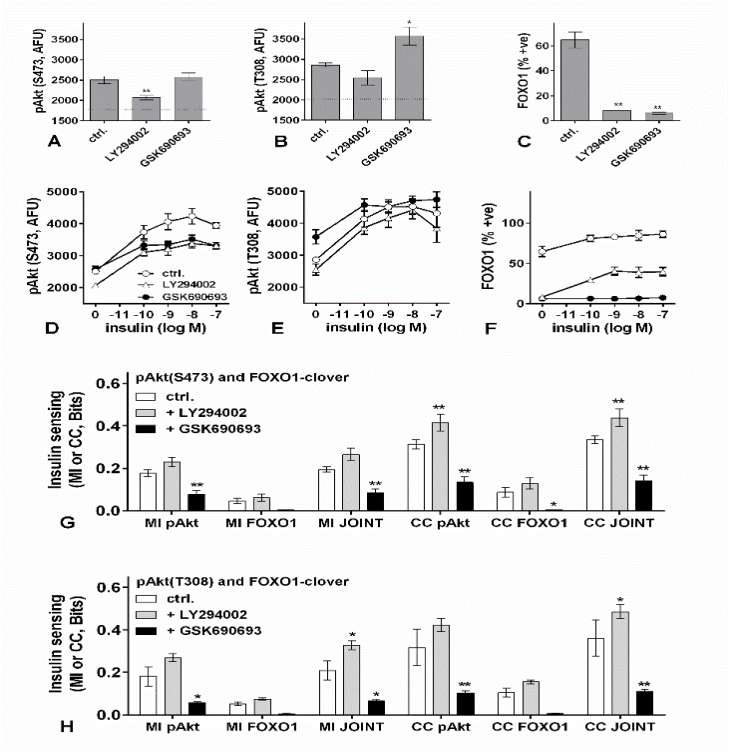

Figure 5. Measuring IR-mediated information transfer to Akt and FOXO1 in fixed cells. A-F: hPod/FOXO1 cells were incubated 60 min with or without LY294002 (10^{-5}M) or GSK690693 ($2x10^{-7}$M) and then stimulated 10 min with insulin (as indicated and in the continued presence of inhibitor) . The % of cells where cytoplasmic FOXO1-clover was >20% greater than the nuclear FOXO1-clover was calculated and is shown as FOXO1 % +ve (C and F). A-C show control data with no insulin, whereas D-F show the full concentration-response curves. CVs calculated for control, LY294002 and GSK690693-treated cells were 3.7±0.2%, 3.2±0.1% and 4.5±0.2% for log-pAkt(S473) and were 3.9±0.2%, 3.9±0.2% and 5.1±0.2% for log-pAkt(T308). One-way ANOVAs and post-hoc Dunnet's tests revealed the effects of GSK690693 on CV to be statistically significant ($P<0.05$) whereas those of LY294002 were not ($P>0.05$). The individual cell measures for the full concentration-response curves were used to calculate MI and CC values for each readout and for the joint measures. To enable the joint measure calculations, pAkt(S473) and FOXO1-clover were quantified in the same cells (panel G) and in parallel experiments, pAkt(T308) and FOXO1-clover were measured in the same cells (panel H). The data shown are means±SEMs (n=4). Two-way ANOVAs for data in G and H revealed insulin and inhibitor as significant sources of variation (irrespective of the Akt phosphorylation site quantified) and post-hoc Dunnett's tests revealed significant differences to the appropriate control measure as indicated (*$P<0.05$, **$P<0.01$).

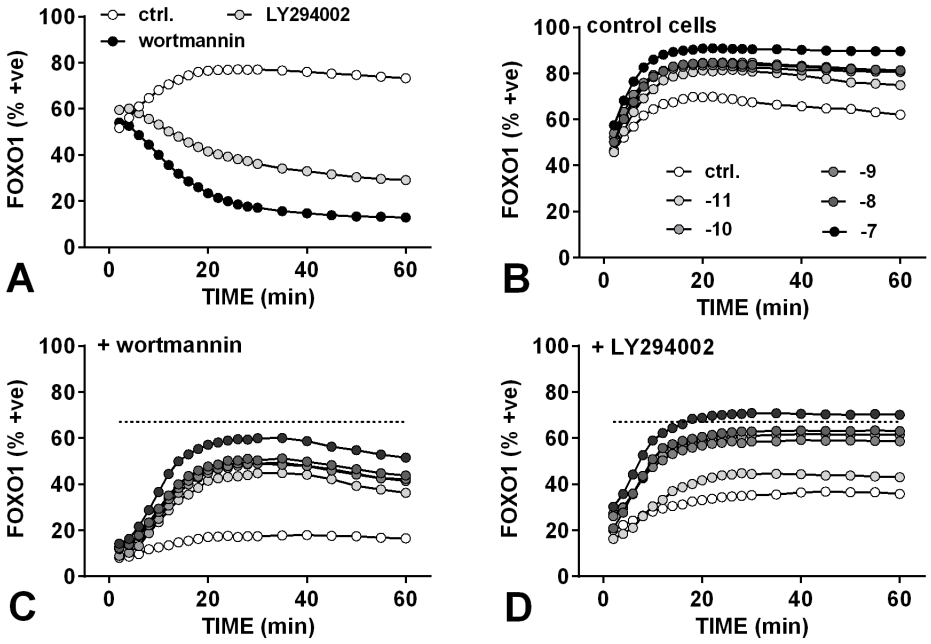

Figure 6. Live cell imaging of FOXO1-clover translocation. A: hPod/FOXO1 cells were imaged at 37ºC during 60 min exposure to wortmannin (10^{-5}M), LY294002 (10^{-5}M) or control medium (starting at t=0) with images captured at 2 min intervals for the first 30 min and at 5 min intervals thereafter. B-D: Cells were pre-treated for 60 min with wortmannin (10^{-5}M, C), LY294002 (10^{-5}M, D) or control medium (B) before 60 min stimulation with insulin at the indicated log M concentration (labels in B apply also to C and D) and in the continued presence of inhibitor. The FOXO1 (% +ve) measure was calculated as for figure 5. For all panels, the data shown are means of population average responses from 4 experiments with SEMs (mostly <10%) omitted for clarity. The horizontal dotted lines in C and D show the mean FOXO1 % +ve value in control cells with no insulin or inhibitor.

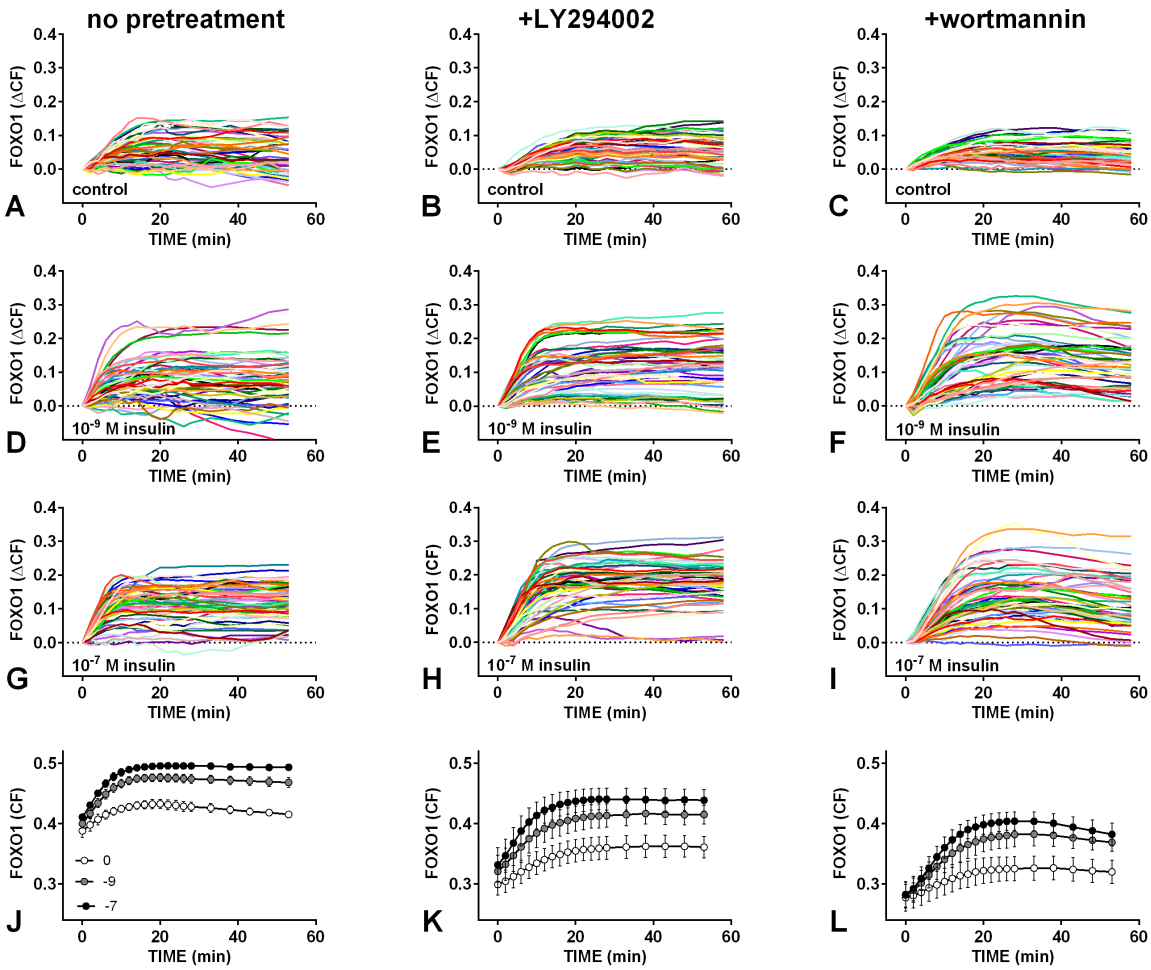

Figure 7. Tracking FOXO1-clover in individual cells. A-I: For the experiments shown in Fig.6B-D, responses were tracked over time as described in the Materials and Methods. To visualise graded responses the nuclear and cytoplasmic FOXO1-clover measures were used to calculate the cytoplasmic fraction (CF), and for each cell the CF at time 0 was subtracted in order to follow changes caused by the treatments (FOXO1 ΔCF). Each panel shows traces for approximately 50 cells receiving the indicated pre-treatment with selected insulin concentrations (0, 10^{-9}M and 10^{-7}M). These are representative of many thousands of cells tracked and visualised in this way. J-L show raw FOXO1 CF values (population averaged data) for the same insulin concentrations, emphasising the fact that the cytoplasmic fraction of FOXO1 was reduced by pre-treatment with LY29402 or wortmannin (compare 0 times in J, K and L). These data are means±SEMs (n=4) and are from the same experiments reported as % +ve in figure 6B-D but with responses to 10^{-11}, 10^{-10} and 10^{-8}M insulin omitted for clarity.

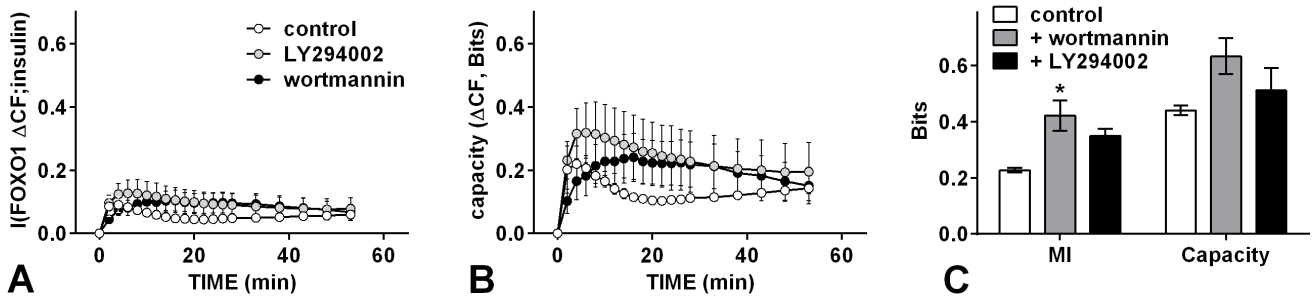

Figure 8. IR-mediated information transfer to FOXO1 in live cells. The tracked cell data (FOXO1-clover ΔCF values from the experiments shown in Fig.6B-D) were analysed to determine MIs and CCs at each time point (A and B, respectively), as well as MI and CC taking the individual cell response trajectories into account (panel C) for control and inhibitor pre-treated cells, as indicated. The values shown are means±SEMs (n=4) in Bits. One-way ANOVA of the MI data ibn C revealed treatment as a significant source of variation and post-hoc Dunnett's tests revealed a significant effect of wortmannin (*P<0.05, compared to control). Treatment was not a significant source of variation for the CC data.